POU2F3-Expressing Small Cell Lung Carcinoma and Large Cell Neuroendocrine Carcinoma Show Morphologic and Phenotypic Overlap

Jimbo, Naoe ; Ohbayashi, Chiho ; Takeda, Maiko ; Fujii, Tomomi ; Mitsui, Suguru ; Tsukamoto, Ryuko ; Tanaka, Yugo ; Itoh, Tomoo ;…

(Citation)
The American Journal of Surgical Pathology,48(1):4-15

(Issue Date)
2024-01

(Resource Type)
journal article

(Version)
Accepted Manuscript

POU2F3-expressing small cell lung carcinoma and large cell neuroendocrine carcinoma show morphologic and phenotypic overlap

Naoe Jimbo, MD, PhD * [a], Chiho Ohbayashi, MD, PhD [b,c], Maiko Takeda, MD, PhD [c], Tomomi Fujii MD, PhD [c], Suguru Mitsui, MD [d], Ryuko Tsukamoto [a], Yugo Tanaka, MD, PhD [d], Tomoo Itoh, MD, PhD, [a] Yoshimasa Maniwa, MD, PhD.[d]

[a] Department of Diagnostic Pathology, Kobe University Graduate School of Medicine, 7-5-2 Kusunoki-cho, Chuo-ku, Kobe City, Hyogo Prefecture 650-0017, Japan.

[b] Department of Diagnostic Pathology, Shinko Hospital, 1-4-47, Wakinohamacho, Chuo-ku, Kobe, 651-0072, Japan.

[c] Department of Diagnostic Pathology, Nara Medical University School of Medicine, Nara, Japan, 840 Shijo-cho, Kashihara, Nara 634-8521, Japan.

[d] Division of Thoracic Surgery, Kobe University Graduate School of Medicine, 7-5-2 Kusunoki-cho, Chuo-ku, Kobe City, Hyogo Prefecture 650-0017, Japan.

***Corresponding author:**

Naoe Jimbo

E-mail: naoe1123@med.kobe-u.ac.jp

Department of Diagnostic Pathology, Kobe University Hospital,

7-5-2 Kusunoki-Cho, Kobe 650-0017, Japan

Tel: +81 78 382 6471

Fax: +81 78 382 6489

This study was supported by JSPS KAKENHI grant numbers JP19K18213 and JP 22K16172.

The authors have disclosed that they have no significant relationships with, or financial interest in, any commercial companies pertaining to this article.

Acknowledgements

We thank biostatisticians in Clinical & Translational Research Center, Kobe University Hospital, who reviewed statistical methods.

Abstract

Considering the differences in protein expression in small cell lung carcinoma (SCLC) by molecular classification, it is likely that there are differences in morphology, but the relationship between molecular classification and morphology has not been examined. Furthermore, there are limited reports concerning this molecular classification for large cell neuroendocrine carcinoma (LCNEC) and SCLC simultaneously. Therefore, we investigated the relationship between immunohistochemistry-based molecular classification and morphology, protein expression, and clinical features of 146 consecutive resection specimens of pulmonary neuroendocrine carcinoma (NEC) focusing mainly on POU2F3, the master transcription factor involved in tuft cell generation. POU2F3-dominant SCLC (n=24) and LCNEC (n=14) showed overlap in cytomorphology, while non-POU2F3-dominant SCLC (n=71) and LCNEC (n=37) showed distinct differences in cytomorphology. Additionally, POU2F3-dominant NEC exhibited significantly more abundant tumor stroma, more prominent nest formation, more frequent bronchial intraepithelial involvement, and less frequent background fibrosis than non-POU2F3-dominant NEC. Immunohistochemically, POU2F3-dominant SCLC and LCNEC were characterized by lower expression of TTF-1, CEA, and neuroendocrine markers, and higher expression of bcl-2, c-Myc, and c-kit. Clinically, POU2F3-dominant NEC had a significantly better prognosis than non-POU2F3-dominant NEC for recurrence-free survival. POU2F3-

dominant NEC had a higher smoking index than non-POU2F3-dominant NEC. POU2F3-dominant NEC forms a unique population, exhibiting intermediate morphological features between SCLC and LCNEC, with distinct protein expression as tuft cell-like carcinoma. Recognition of this unique subtype may provide clues for solving the long-standing issues of NEC and appropriate therapeutic stratification. It is important to accurately identify POU2F3-expressing carcinomas by immunohistochemistry and to analyze their clinicopathological features.

Keywords: POU2F3, tuft cell, small cell lung carcinoma, large cell neuroendocrine carcinoma, molecular classification

Abbreviation

small cell lung carcinoma (SCLC)

SCLC dominantly expressing ASCL1 (SCLC-A)

SCLC dominantly expressing NEUROD1 (SCLC-N)

neuroendocrine (NE)

SCLC dominantly expressing POU2F3 (SCLC-P)

SCLC dominantly expressing YAP (SCLC-Y)

large cell neuroendocrine carcinoma (LCNEC)

squamous cell carcinoma (SQCC)

neuroendocrine carcinoma (NEC)

World Health Organization (WHO)

Immunohistochemistry (IHC)

Synaptophysin (SYN)

Chromogranin A(CGA)

cytokeratin (CK)

tumor proportion score (TPS)

triple-negative (TN)

non-small cell lung carcinoma (NSCLC)

triple-negative SCLC (SCLC-TN)

LCNEC dominantly expressing ASCL1 (LCNEC-A)

LCNEC dominantly expressing NEUROD1 (LCNEC-N)

LCNEC dominantly expressing POU2F3 (LCNEC-P)

triple-negative LCNEC (LCNEC-TN)

NEC dominantly expressing ASCL1 (NEC-A)

NEC dominantly expressing NEUROD1 (NEC-N)

NEC dominantly expressing POU2F3 (NEC-P)

triple-negative NEC (NEC-TN)

recurrence free survival (RFS)

overall survival (OS)

Introduction

Recently, small cell lung carcinoma (SCLC) has been classified into four types by the relative expression of four transcriptional key factors (ASCL1, NEUROD1, POU2F3, and YAP1) [1]. SCLC dominantly expressing ASCL1 (SCLC-A) or NEUROD1 (SCLC-N) were recognized as neuroendocrine (NE)-phenotype SCLC, whereas SCLC dominantly expressing POU2F3 (SCLC-P) were recognized as non-NE phenotype SCLC. SCLC-A and SCLC-N usually express TTF-1 at high levels, whereas SCLC-P showed no or low expression of TTF-1 [2, 3]. YAP1 (SCLC-Y) was also initially recognized as a non-NE phenotype SCLC, but SCLC-Y is a cell-line-based concept considered inapplicable to primary SCLC [2-7]. For each subtype, different

effects of immunotherapy or molecular-targeted therapy in models or patients have been suggested [4,8,9].

POU2F3 is a lineage-defining transcription factor involved in the generation of tuft cells, which are epithelial chemosensory cells distributed in many organs, including the respiratory tract [10]. Huang et al. reported the first tuft cell-like cancer as a variant of SCLC that express POU2F3[8], and since then, there has been increased attention to POU2F3. POU2F3-expressing carcinoma has been identified in not only SCLC (7–12%) [2,3], but also pulmonary large cell neuroendocrine carcinoma (LCNEC) (12-20%) [3,11], and pulmonary squamous cell carcinoma (SQCC) and adenocarcinoma (<5%) [11]. In extrapulmonary regions, POU2F3-expressing carcinoma has also been reported in the thymus [11,12], skin [13], prostate [14], genital organs, gynecological ducts, and breast [15,16]. Recent studies have shown significantly higher expression of bcl-2 and c-kit in POU2F3-expressing carcinoma, regardless of organ or histological type [15, 16]. Additionally, POU2F3-expressing SCLC and LCNEC, but not SQCC, also overexpressed c-Myc [3].

No large cohort studies have examined the relationship between molecular biological classification and morphology. Given the differences in protein expression by molecular type, it is not surprising that there were differences in morphology. Another question is what would result when this molecular biological classification is applied to LCNEC. Therefore, we determined the molecular classification of LCNEC and SCLC, and examined whether there are differences between molecular classification and morphology or protein expression, focusing mainly on POU2F3. This is the first attempt to combine surgical cases of SCLC and LCNEC and to evaluate the relationship between molecular biological subtypes and morphology.

Material and Methods

Sample

This study was approved by the Ethics Committee of Kobe University Hospital (No. B220045). In total, 146 consecutive surgically resected high-grade neuroendocrine carcinoma (NEC) samples, including SCLC and LCNEC, were obtained at Kobe University Hospital from 2000 to 2022 and at Nara Medical University from 2016 to 2022.

Morphology review

The histological diagnosis of SCLC and LCNEC was based on the fifth World Health Organization (WHO) classification of Tumors[17]. All cases were reviewed and reorganized into SCLC and LCNEC by two pathologists specializing in lung cancer (NJ and CO, respectively). An average of 4.1 hematoxylin and eosin-stained specimens per case were evaluated. We agreed with the decision of SCLC or LCNEC in most cases (128 of 146 cases), while we decided on the final diagnosis with discussion for disagreement cases. Finally, it was determined that 95 cases were SCLC and 51 cases were LCNEC. The cytomorphological score (0–12) was defined as the sum of six cytomorphological parameters: nuclear size, nuclear molding, chromatin pattern, length-to-width ratio, cytoplasm, and nucleoli, which were scored as 0, 1, and 2, respectively, with lower values indicating more SCLC-like features. The degree of tumor stroma and nest formation were evaluated on a 3-point scale (0, 1, and 2). Cytomorphological score and the degree of tumor stroma and nest formation were each evaluated by two pathologists, and the average of the values was scored. In addition, comedo necrosis, bronchial intraepithelial involvement, and background lung fibrosis were evaluated on a 2-point scale (0 = no, 1 = yes). Bronchial intraepithelial involvement is a tumor invasion into

the bronchus or bronchioles inside or outside the primary tumor. The detailed methods for morphological evaluation are described in Supplemental Digital Content 1.

Immunohistochemistry (IHC) and IHC assessment

In this study, a total of 18 types of antibodies, ASCL1, NEUROD1, POU2F3, YAP1, Synaptophysin (SYN), Chromogranin A(CGA), CD56, INSM1, TTF1, CEA, bcl-2, c-Myc, c-kit, CD5, p40, cytokeratin (CK) 5/6, Rb1, and PD-L1, were used. Protein expression was determined using Ventana BenchMark GX (Roche, Basel, Switzerland), BOND-MAX/BOND-III (Leica, Deer Park, US), or Dako Autostainer Link 48 (Agilent Technologies, Santa Clara, US) automated immunostainer.

A total of 2626 sections were evaluated for immunostaining on a formalin-fixed paraffin-embedded block, of which 1509 sections (57%) were evaluated on whole slides and the remaining 1117 sections (43%) on spiral arrays. Whole slides were used in all cases for YAP1 and p40, as well as in more than 90% of cases for POU2F3, SYN, CGA, and CD56. Spiral tissue arrays were chosen instead of conventional core tissue microarrays to reduce the effects of heterogeneity. The methods for constructing a spiral tissue array have been described previously [18]. The expression of Rb1 was scored as retain or loss. PD-L1 expression was

determined by tumor proportion score (TPS) and defined as positive if TPS ≥1%. The other 16 markers were evaluated using the H-score. H-score (0–300) is defined as the multiplication of intensity (0, 1=weak, 2=moderate, 3=strong) and proportion (0–100%) of the expressed tumor cells according to a previously reported study [2, 3]. In addition, the NE-score was calculated as the average of the H-scores of the four classical NE markers (SYN, CGA, CD56, and INSM1), with values ranging from 0-300 [2,3]. The marker showing the highest H-score of 50 or more among the three transcriptional markers, ASCL1, NEUROD1, and POU2F3, was defined as the dominant type. The triple-negative (TN) group was defined as cases in which ASCL1, NEUROD1, and POU2F3 were all expressed to a score of less than 50. Only the SCLC component was scored in cases of combined SCLC with non-small cell lung carcinoma (NSCLC) including LCNEC, while only the LCNEC components were scored in cases of combined LCNEC and non-NEC NSCLC. IHC details are described in Supplemental Digital Content 2.

According to whether they were SCLC or LCNEC and IHC-based molecular classification, eight groups were established: SCLC-A, SCLC-N, SCLC-P, triple-negative SCLC (SCLC-TN), LCNEC dominantly expressing ASCL1 (LCNEC-A), LCNEC dominantly expressing NEUROD1 (LCNEC-N), LCNEC dominantly expressing POU2F3 (LCNEC-P), and triple-negative LCNEC (LCNEC-TN). As the integration of SCLC and LCNEC, NEC dominantly

expressing ASCL1 (NEC-A), NEC dominantly expressing NEUROD1 (NEC-N), NEC dominantly expressing POU2F3 (NEC-P), and triple-negative TN (NEC-TN) were defined.

Statistical analyses

Statistical analyses between POU2F3-dominant vs. POU2F3-non-dominant type (SCLC, LCNEC, and NEC, respectively) were performed in patient characteristics, prognosis, morphological features, and IHC. Additionally, statistical analyses between SCLC vs. LCNEC, SCLC-P vs. LCNEC-P, and SCLC-non-P vs. LCNEC-non-P with respect to patient characteristics, morphological features, and IHC are also included. Comparisons of variables for patient characteristics and pathological features were made using the Mann-Whitney or Fisher's exact test. The correlation between the expression of four novel transcriptional markers (ASCL1, NEUROD1, POU2F3, and YAP1) and each marker's expression as measured by IHC was examined using the Spearman correlation coefficient.

Recurrence-free survival (RFS) was defined as the time from the date of surgery to that of recurrence or death by any cause. Overall survival (OS) was defined as the time from the date of surgery until death by any cause or until the last follow-up visit. RFS and OS were evaluated using the Kaplan–Meier method, and differences in survival curves were assessed using the log-

rank test. Statistical analyses were performed using EZR version 1.40 (Saitama Medical Center, Jichi Medical University, Saitama, Japan) and R (The R Foundation for Statistical Computing, Vienna, Austria).

Statistical significance was set at $p < 0.05$. All p-values are two-sided and not adjusted for multiple testing.

Results

Group configuration and the number of cases in each group

As shown in Table 1, based on our criteria based on IHC, SCLC-P, SCLC-A, SCLC-N, SCLC-TN, LCNEC-P, LCNEC-A, and LCNEC-TN were assigned to 24, 49, 20, 2, 14, 27, and 10 cases, respectively. None of the cases corresponded to LCNEC-N. The number of NEC-P, NEC-A, NEC-N, and NEC-TN cases were 38, 76, 20, and 12, respectively.

Patient Characteristics

As shown in Table 2, 146 patients, including 126 men (86%) and 20 women (14%), with a median age of 73 (range 40–89) years, were selected as subjects. Almost all but three had a history of smoking, with a median smoking history of 51 pack-years (range 0–300). All NEC-P patients were smokers. There were significant differences in the smoking index between LCNEC-P vs. LCNEC-non-P and NEC-P vs. NEC-non-P (p=0.009, 0.02, respectively). In SCLC, the frequency of stage I SCLC-P (71%) was significantly higher than that of SCLC-non-P (42%) (p=0.02). Overall, 48% of the patients received postoperative chemotherapy, but significantly more patients with SCLC (55%) received chemotherapy than those with LCNEC (35%) (p=0.04). Forty-eight of 146 patients (33%) had NEC combined with NSCLC. There was no significant difference in the number of cases with combined histology with SQCC between NEC-P and NEC-non-P. However, when evaluated within combined NEC, all combined NEC-P (100%, 8/8) had SQCC, while only half of combined NEC-non-P had SQCC (50%, 20/40).

Prognosis

There was a significant difference in RFS among the four groups (SCLC-P, SCLC-non-P, LCNEC-P, and LCNEC-non-P) (p=0.046), whereas there was no significant difference in OS (p=0.224) (Figure 1a, b). SCLC-P tended to have a better prognosis for RFS than SCLC-non-P

(p=0.057), but there was no significant difference between LCNEC-P and LCNEC-non-P (p=0.210) (Figure 1a). There were no significant differences in OS between SCLC-P vs. SCLC-non-P (p=0.259) and LCNEC-P vs. LCNEC-non-P (p=0.403) (Figure 1b). NEC-P had a significantly better prognosis in terms of RFS than NEC-non-P (p=0.026), but no significant difference in OS (p=0.172) (Figure 1c, d). There were no significant differences in RFS and OS between the SCLC-P and LCNEC-P (p=0.414 and p=0.372, respectively) (data not shown).

Morphological features

The results of morphological features are shown in Table 3 and Figure 2. As for cytomorphological scores (0–12), there was a significant difference both SCLC-P (median=5, red line in Figure 2) vs. SCLC-non-P (3) and LCNEC-P (8) vs. LCNEC-non-P (11) (p<0.001 for both). In contrast, there was no significant difference between NEC-P (6.3) vs. NEC-non-P (4). Although there was still a significant difference between SCLC-P and LCNEC-P (p<0.001), interestingly, the scatter dot plots of the cytomorphological score in Figure 2a showed an overlap between SCLC-P and LCNEC-P. On the other hand, there was an even greater difference between SCLC-non-P and LCNEC-non-P, evident in the same scatter dot plots.

These indicated that SCLC-P exhibited more LCNEC-like cytomorphology, while LCNEC-P was closer to SCLC-like cytomorphology.

As for tumor stroma, nest formation, and comedo necrosis, they were significantly more prominent in SCLC-P than in SCLC-non-P (p <0.001 for all three). Among LCNEC, only tumor stroma was more significantly prominent in LCNEC-P than in LCNEC-non-P (p <0.001). In an integrated analysis of SCLC and LCNEC, NEC-P showed significantly more abundant tumor stroma and nest formation than NEC-non-P (p <0.001, 0.012, respectively). These three features were significantly more prominent in LCNEC than in SCLC (p <0.001, <0.001, 0.003, respectively).

The frequency of bronchial intraepithelial involvement was 25%, which was the same rate for both in SCLC and LCNEC. Notably, it was significantly higher in SCLC-P (46%) than SCLC-non-P (18%), LCNEC-P (57%) than LCNEC-non-P (14%), and NEC-P (50%) than NEC-non-P (17%) (p=0.01, 0.003, <0.001, respectively). Background fibrosis was significantly lower in SCLC-P (4%) than in SCLC-non-P (37%) and significantly lower in NEC-P (8%) than in NEC-non-P (30%) (p =0.002, 0.007, respectively). Of the 146 cases, 16 cases (11%) required discussion to distinguish SCLC from LCNEC, 10 cases of which were classified as NEC-P.

Approximately one-fourth (26%) of the type NEC-P cases required discussion, significantly more frequently than NEC-non-P (6%) (p =0.002).

Representative pathological findings

As shown in a typical representative example (Figure 3), most SCLC-A showed a diffuse growth pattern with extensive coagulation necrosis, whereas SCLC-P formed relatively round nests with comedo necrosis and wider stroma with prominent inflammation. Most SCLC-A showed small cell cytology, and most LCNEC-A showed non-small cell cytology, while SCLC-P had intermediate features between small cell and non-small cell, for example, slightly larger nuclei, slightly more prominent cytoplasm, slightly more prominent nucleoli, and slightly coarser chromatin. Most LCNEC-P exhibited morphological features that were more similar to SCLC-P than to LCNEC-A.

In NEC-P, approximately half of the cases showed bronchial intraepithelial involvement of tumor cells in the non-neoplastic ciliated epithelium (Figure 4 a,b). Interestingly, one case of SCLC-P showed not only bronchial intraepithelial involvement but also a single to several layers of tumor cells under non-neoplastic pneumocytes, partially resembling the lepidic growth

of adenocarcinoma (Figure 4c). Double staining indicated POU2F3-positive tumor cells (red) extending under the TTF-1-positive alveolar epithelium (blue) (Figure 4d).

IHC

H-score of antibodies, Rb1 expression, and PD-L1 expression in each case are shown in the heat map (Figure 5). In addition, detailed IHC results including *p*-value are presented in Supplemental Digital Content 3. The heatmap of IHC clearly showed similarities in protein expression between SCLC-P and LCNEC-P, with lower expression of classical NE markers (although CD56 remained relatively expressed among these), TTF-1, and CEA, and higher expression of YAP1, bcl-2, c-Myc, and c-kit. At the same time, IHC heatmap showed significant protein expression differences between SCLC-P vs. SCLC-non-P and LCNEC-P vs. LCNEC-non-P.

In statistical analysis (each *p*-values are shown in Supplemental Digital Content 3), NEC-P had significantly lower expression of classical NE markers, TTF-1, and CEA, and significantly higher expression of YAP1, bcl-2, c-Myc, and c-kit than NEC-non-P ($p < 0.001$ for all). Expression of CD5, p40, and CK5/6 was observed in 27, 20, and 18 cases, respectively.

There was no significant difference in CD5 expression between NEC-P and NEC-non-P. The overall expression of p40 and CK5/6 was very low, but the expression of p40 and CK5/6 was significantly higher in NEC-P than in NEC-non-P (p=0.043, <0.001, respectively). The only significant difference between SCLC-P and LCNEC-P was bcl-2 expression (higher in SCLC-P, p<0.001).

Rb1 loss was observed in 93% of SCLC and was significantly more frequent than LCNEC (43%) (p<0.001). SCLC-P had significantly fewer cases (79%) showing Rb1 loss than SCLC-non-P (97%) (p=0.01), whereas LCNEC-P tended to have more cases with Rb1 loss (64%) than LCNEC-non-P (35%) (p=0.11). Between SCLC-P and LCNEC-P, there was no significant difference in the frequency of Rb1 loss (79% vs. 64%), whereas there was a significant difference between SCLC-non-P vs LCNEC-non-P (97% vs. 35%) (p<0.001). PD-L1 expression (TPS>1%) was found in 16% of all cases. There was no significant PD-L1 expression between any two groups.

Correlation coefficients for each marker

Correlations between the expression of the four novel transcriptional markers and various proteins were examined in all the cases (Supplemental Digital Content 4). Six combinations

with relatively strong correlations above ρ=0.6 or below ρ=-0.6 were ASCL1 and SYN (0.60), ASCL1 and INSM1(0.62), POU2F3 and SYN (-0.67), POU2F3 and c-kit (0.60), YAP1 and SYN (-0.64), and YAP1 and INSM1(-0.63).

Scatter plot of cytomorphological score and NE-score

Each case was plotted so that the cytomorphological score was on the horizontal axis (0–12) and NE-score (0–300) was on the vertical axis (Figure 6). SCLC-P was indicated by red squares, LCNEC-P by blue squares, SCLC-non-P by black circles, and LCNEC-non-P by green circles, with the respective 95% confidence intervals indicated by each colored thick solid line. Interestingly, the majority of SCLC-P and LCNEC-P were plotted in the borderline region between SCLC and LCNEC in the low NE expression area and the 95% confidence intervals for SCLC-P and LCNEC-P overlapped, suggesting that NEC-P is difficult to determine whether they are SCLC or LCNEC. Conversely, the plotted areas for SCLC-non-P and LCNEC-non-P differed, and the 95% confidence intervals for SCLC-P and LCNEC-P overlapped little. In addition, the thin black lines showed the 95% confidence intervals for SCLC-A, SCLC-N, and SCLC-TN, and the thin green lines showed the 95% confidence intervals for LCNEC-A and

LCNEC-TN. The distribution of SCLC-N is similar to that of SCLC-A, and the distribution of LCNEC-TN overlaps that of LCNEC-P.

Discussion

This study is the first large cohort to examine the relationship between IHC-based molecular biological classification and morphological or immunohistochemical features using 146 resected samples, including SCLC and LCNEC. The most striking and novel finding was that NEC-P formed a distinctly different group in several respects, showing not only unique protein expression as a tuft cell-like signature but also intermediate morphology between SCLC and LCNEC and favorable prognosis for RFS. Furthermore, NEC-P was characterized by a higher smoking index, higher frequency of bronchial intraepithelial involvement, lower frequency of background fibrosis, and higher frequency of combined NEC with SQCC.

In our cohort, SCLC-non-P and LCNEC-non-P showed clear cytomorphological differences. Conversely, the cytomorphological features of SCLC-P and LCNEC-P overlapped. Not only

that, but SCLC-P also exhibited features usually considered prominent in LCNEC, such as abundant stroma, nest formation, and comedo necrosis, suggesting difficulties separating SCLC and LCNEC. Historically, pure SCLC was recognized as having several distinct morphological features, including lymphocyte-like, fusiform, and polygonal [19] or oat cell and intermediate [20], but these have disappeared due to crush artifacts and poor fixation, as well as the low reproducibility of diagnostic concordance rates, leaving only pure SCLC and combined SCLC since the third edition of WHO classification [21]. In 1991, the new concept of LCNEC was introduced [22]. SCLC and LCNEC are distinguished by morphological findings; however, the difficulty in differentiating between SCLC and LCNEC remains a well-recognized but serious issue for pathologists and clinicians for a long time because it is directly related to the problem of different treatment strategies for SCLC and LCNEC [23].

On the contrary, it has also been recognized that there is a borderline high-grade NEC showing intermediate morphological features between SCLC and LCNEC or cytological overlap between these two [24-27]. Hiroshima et al. reported that borderline high-grade NEC had features of both SCLC (small amount of cytoplasm, high nucleus-to-cytoplasmic ratio, finely granular chromatin, and inconspicuous nucleoli) and LCNEC (polygonal shape, large nuclei, and neuroendocrine growth patterns). Interestingly, borderline high-grade NEC often showed synaptophysin (-), chromogranin A (-), CD56 (+), and TTF-1 (-) expression, which is

consistent with the characteristics of the majority of NEC-P in our cohort [28]. Based on the above, we believe that histological variety in SCLC is indeed present, and that the majority of NEC-P cases show intermediate morphological features between SCLC and LCNEC and may correspond to fusiform, polygonal, or intermediate types in the old histological classification.

The frequency of bronchial intraepithelial involvement was significantly higher in the NEC-P (50%) than in the NEC-non-P (17%) (p<0.001). Additionally, one unique NEC-P case showed bronchial intraepithelial involvement as well as beneath the alveolar epithelium. Kojima et al. reported “bronchial intraepithelial tumor spread” as a unique form of tumor invasion found in 19% (9/47) cases of NEC [29]. They showed that NEC with this pattern was associated with a high recurrence rate (89%) and a high frequency of positive surgical margins of the bronchus (44 %). Considering the high frequency of bronchial intraepithelial involvement in NEC-P, intraoperative diagnosis of the cut end of the bronchus and sleeve lobectomy may be required in NEC-P. Although it is unclear whether the bronchial intraepithelial involvement represents a primary lesion (NEC in situ) or invasion by underlying cancer [30], recognition of this feature is essential not only to determine the appropriate surgical approach, but also as a clue to the authenticity of the precursor lesion of NEC.

Most cases of NEC-P showed emphysema and respiratory bronchiolitis with prominent macrophages, strongly suggesting the influence of smoking; however, background fibrosis was significantly less common in NEC-P (8%) than in NEC-non-P (30%) (p=0.007). The relationship between background and subtype has not been previously noted, and more cases including the effect of smoking need to be accumulated.

In this cohort, NEC-P had a significantly better prognosis concerning RFS than NEC-non-P, and SCLC-P tended to have a better prognosis concerning RFS than SCLC-non-P. The favorable results of SCLC-P may be associated with a higher proportion of stage I or a lower frequency of background fibrosis. We previously reported that NEC with low NE or INSM1 negative have a better prognosis [18,31], which may be related to the possibility that NEC-P are frequently included in these groups. Some reports found no significant difference in prognosis between SCLC-P and SCLC-non-P [3, 4], while others reported that SCLC-P has a favorable prognosis [32]. The exact relationship between molecular classification and prognosis needs to be investigated through more extensive studies, considering circumstances such as background lung disease.

At the protein level, SCLC-P and LCNEC-P shared protein expression features (TTF-1^{low}, NE markers ^{low}, CEA ^{low}, bcl-2 ^{high}, c-Myc ^{high}, and c-kit ^{high}). These phenotypical features (particularly TTF-1^{low}, NE markers ^{low}, bcl-2 ^{high}, c-Myc ^{high} , and c-kit ^{high}) were reproducible results, consistent with the previous reports on POU2F3-positive SCLC and LCNEC [2,3,33]. As novel findings, significantly lower expression of CEA was found in NEC-P. The expression of p40 and CK5/6 was very low, but the expression of p40 and CK5/6 was significantly higher in NEC-P than in NEC-non-P. Notably, there was the strongest correlation between expression between POU2F3 and SYN (ρ = -0.67), but also a relatively strong correlation between POU2F3 and c-kit (ρ = 0.6).

Regarding the frequency of Rb1 loss, there was no significant difference between SCLC-P and LCNEC-P, whereas there was a significant difference between SCLC-non-P and LCNEC-non-P (p<0.001). LCNEC-P (64%) tended to have a higher frequency of Rb1 protein loss than LCNEC-non-P (35%) (p=0.11). The mutation rate of *Rb1* was reported to be significantly higher in tuft cell-like LCNEC than in non-tuft cell-like LCNEC (p=0.0002) [11], consistent with our results.

POU2F3-expressing carcinoma is recognized as tuft cell-like carcinoma [8, 15, 16], although it remains unclear whether tuft cells are the origin of POU2F3-expressing carcinoma [3]. Tuft cell-like carcinoma have been reported in various histotypes and organs, with co-expression of c-kit and bcl-2 [15,16,33]. Among these carcinoma, pulmonary tuft cell-like SCLC and LCNEC (but not SQCC) also showed high expression of c-Myc [3,33]. POU2F3 is a master regulator of tuft cells, which are epithelial chemosensory cells with long and thick microvilli, distributed in many organs, including the pancreatic duct, respiratory tract, intestine, salivary gland, gallbladder, and urethra. Tuft cells sense external stimuli through taste-like signaling pathways and generate epithelium-specific outputs such as interleukin-25, eicosanoids involved in allergic immunity, and acetylcholine [10].

Goldfarbmuren et al. created a comprehensive atlas of tracheal epithelial cell types, including rare cell types (tuft, pulmonary neuroendocrine, and ionocyte), by RNA sequencing of single cells. Detailed studies have revealed that rare cells are derived from basal cells, with tuft cell-like cells being the closest to basal cells and likely progenitors of pulmonary neuroendocrine cells and ionocytes [34]. As a “lineage ambiguity”, tuft cell-like tumors have been shown to co-express neuroendocrine and squamous differentiation markers [33]. A specific relationship between POU2F3 and squamous differentiation (higher frequency of combined NEC with

SQCC and higher expression of p40 and CK 5/6 in NEC-P) was also observed in our cohort, which may be related to similar “lineage ambiguity” in NEC-P.

Considering lower NE expression, relationship with squamous differentiation, and unique clinicopathological features in NEC-P, it is seemingly difficult to place NEC-P in the category of “neuroendocrine carcinoma”. However, the secretory potential of tuft cells may allow NEC-P to be classified as “neuroendocrine carcinoma” in a broad sense. The high rate of Rb1 abnormalities in LCNEC-P, as in SCLC-P, may also be evidence of NEC-P being a “neuroendocrine carcinoma”. Thus, the question remains as to what defines a "neuroendocrine carcinoma" and this dilemma needs to be clarified in the future.

Loss of YAP1 has been reported to define neuroendocrine differentiation in lung tumors [5 ito]. Compared with previous reports, the expression of YAP1 in SCLC-P in our cohort was generally higher [2]. This might be because all cases of YAP1 and almost all cases of POU2F3 were tested on whole slides, as well as differences in antibodies or IHC protocols. However, under the assumption that the loss of YAP1 defines neuroendocrine differentiation, our results may be more reasonable given the low NE expression characteristic of NEC-P. SCLC-Y is likely to have been established from a minor component of non-NE cells exhibiting YAP1 in

classic SCLC [6,7], so it should not be applied to primary SCLC. However, YAP1 also contributes to cancer cell proliferation as an effector of the Hippo pathway in various cancers, and high YAP1 expression is associated with drug resistance [35]. Additionally, nuclear overexpression of YAP is associated with poor prognosis in NSCLC [36]. Considering these aspects, confirming YAP1 expression in each case may be crucial for treatment strategy considerations.

The treatment of NSCLC is rapidly becoming increasingly personalized. In contrast, the treatment strategy for SCLC without the appropriate driver gene abnormality has not changed significantly for approximately 40 years. Despite extensive basic and clinical research, little progress, such as prolonged OS with the addition of anti-PD-L1 antibody to chemotherapy in advanced SCLC, has been made [37,38]. One reason targeted therapy for SCLC has not been effective may be inadequate stratification. The high expression of c-Myc, bcl-2, and SLFN11 are candidate biomarkers for the efficacy of Aurora A kinase inhibitors, bcl-2 inhibitors, and PARP inhibitors, respectively [4, 16, 39, 40]. The expression of mRNA *SLFN11* is significantly higher in tuft cell-like tumors of the lung, prostate, and breast [16]. Most NEC-P correspond to a distinct population with high expression of c-Myc, bcl-2, and SLFN11, and may respond

specifically to such molecularly targeted therapies. In thymic SQCC, *c-kit* mutations are found in approximately 10% of cases, so it may be necessary to search for *c-kit* mutations to identify therapeutic targets. Regarding the various peculiarities of NEC-P, it may be required to consider whether conventional surgical indications, surgical methods, and chemotherapy for SCLC are appropriate and to reconsider treatment strategies. POU2F3-IHC can be easily performed in any laboratory, and its routine use is desirable.

The limitations of this study are that this study is limited to IHC testing, there may be differences at the genetic level. There is no fixed method for determining the dominant type when two or more types are expressed or when a low expression is observed; therefore, the results may differ slightly depending on the method. The criteria for determining molecular classifications may also need to be aligned. Another limitation is the bias caused by limiting to surgical materials. The present study was limited to surgical materials with fewer artifact effects for detailed morphological review, but a more extensive study of non-resected cases is also needed. In addition, NEC-TN cannot be fully discussed because of the small number of cases.

In summary, NEC-P exhibited a distinct population that mainly showed intermediate morphological features between SCLC and LCNEC, better prognosis than NEC-non-P, and

specific protein expression pattern (TTF-1^{low}, NE markers ^{low}, CEA ^{low}, bcl-2 ^{high}, c-Myc ^{high}, and c-kit ^{high}) as tuft cell-like signatures. The clinical significance of NEC-P separation is important because of the possibility of different therapeutic responses. A certain number of complex cases that are difficult to distinguish between SCLC vs. LCNEC or NEC vs. non-NEC, are likely to be NEC-P. We believe that accurate identification of this distinct subtype and analysis of clinicopathologic features are clues to solving several issues associated with NEC.

Reference

1. Rudin CM, Poirier JT, Byers LA, et al. Molecular subtypes of small cell lung cancer: a synthesis of human and mouse model data. *Nat Rev Cancer*. 2019;19:289–297.
2. Baine MK, Hsieh MS, Lai WV, et al. SCLC Subtypes Defined by ASCL1, NEUROD1, POU2F3, and YAP1: A Comprehensive Immunohistochemical and Histopathologic Characterization. *J Thorac Oncol*. 2020;15:1823–1835.
3. Baine MK, Febres-Aldana CA, Chang JC, et al. POU2F3 in SCLC: Clinicopathologic and Genomic Analysis With a Focus on Its Diagnostic Utility in Neuroendocrine-Low SCLC. *J Thorac Oncol*. 2022;17:1109–1121.

4. Gay CM, Stewart A, Park E, et al. Patterns of transcription factor programs and immune pathway activation define four major subtypes of SCLC with distinct therapeutic vulnerabilities. *Cancer Cell*. 2021;39:346–60 e7.

5. Ito T, Matsubara D, Tanaka I, et al. Loss of YAP1 defines neuroendocrine differentiation of lung tumors. *Cancer Sci*. 2016;107:1527–1538.

6. Matsuoka R, Kawai H, Ito T, et al. Determining Whether YAP1 and POU2F3 Are Antineuroendocrine Factors. *J Thorac Oncol*. 2022;17:1070–1073.

7. Kawai H, Matsuoka R, Ito T, et al. Molecular Subtypes of High-Grade Neuroendocrine Carcinoma (HGNEC): What is YAP1-Positive HGNEC? *Front Biosci (Landmark Ed)*. 2022;27:108.

8. Huang YH, Klingbeil O, He XY, et al. POU2F3 is a master regulator of a tuft cell-like variant of small cell lung cancer. *Genes Dev*. 2018;32:915–928.

9. Poirier J, George J, Owonikoko T, et al. New Approaches to SCLC Therapy: From the Laboratory to the Clinic. *J Thorac Oncol*. 2020;15(4):520–540.

10. O'Leavy, CE, Schneider C, and Locksley RM. Tuft Cells-Systemically Dispersed Sensory Epithelia Integrating Immune and Neural Circuitry. *Annu Rev Immunol* 2019;37:47-72.

11. Yamada Y, Simon-Keller K, Belharazem-Vitacolonnna D, et al. A Tuft Cell-Like Signature Is Highly Prevalent in Thymic Squamous Cell Carcinoma and Delineates New

Molecular Subsets Among the Major Lung Cancer Histotypes. *J Thorac Oncol*. 2021;16:1003–1016.

12. Yamada Y, Sugimoto A, Hoki M et al. POU2F3 beyond thymic carcinomas: expression across the spectrum of thymomas hints to medullary differentiation in type A thymoma. *Virchows Arch*. 2022;480:843–851.

13. Chen H, Yang J, Wu W. Seven key hub genes identified by gene co-expression network in cutaneous squamous cell carcinoma. *BMC Cancer*. 2021; 21:852.

14. Brady NJ, Bagadion AM, Singh R et al. Temporal evolution of cellular heterogeneity during the progression to advanced AR-negative prostate cancer. *Nat Commun*. 2021;12:3372.

15. Koh J, Kim H, Moon K-C et al. Molecular classification of extrapulmonary Neuroendocrine carcinoma with emphasis on POU2F3-positive Tuft Cell Carcinoma. *Am J Surg Pathol*. 2023;47:181-193.

16. Yamada Y, Bohnenberger H, Kriegsmann M, et al. Tuft cell-like carcinomas: novel cancer subsets present in multiple organs sharing a unique gene expression signature. *Br J Cancer*. 2022;127:1876–1885.

17. Beasley MB, Brambilla E, MacMahon H, et al. Small cell lung carcinoma. In: WHO classification of Tumors. Lyon, France: International Agency for Reasearch on Cancer; 2021.

18. Minami K, Jimbo N, Tanaka Y, et al. Insulinoma-associated protein 1 is a prognostic biomarker in pulmonary high-grade neuroendocrine carcinoma. *J Surg Oncol*. 2020;122:243–253.

19. Kreyberg L, Liebow AA, Uehlinger EA. International Histological Classification of Tumours: No. 1. Histological Typing of Lung Tumours (ed 1). Geneva, World Health Organization, 1967.

20. Kreyberg L, Liebow AA, Uehlinger EA. International Histological Classification of Tumours: No. 1. Histological Typing of Lung Tumours (ed 2). Geneva, World Health Organization, 1981.

21. Travis WD, Colby TV, Corrin B, et al. World Health Organization International Histological Classification of Tumours: Histological Typing of Lung and Pleural Tumours (ed 3). Berlin, Springer Verlag, 1999.

22. Travis WD, Linnoila RI, Tsokos MG, et al. Neuroendocrine tumors of the lung with proposed criteria for large-cell neuroendocrine carcinoma. An ultrastructural,

immunohistochemical, and flow cytometric study of 35 cases. *Am J Surg Pathol*. 1991;15:529–553.

23. Travis WD, Gal AA, Colby TV, et al. Reproducibility of neuroendocrine lung tumor classification. *Hum Pathol*. 1998;29:272–279.

24. Hiroshima K, Iyoda A, Sida T, et al. Distinction of pulmonary large cell neuroendocrine carcinoma from small cell lung carcinoma: a morphological, immunohistochemical, and molecular analysis. *Mod Pathol*. 2006;19:1358–1368.

25. Hiroshima K, Mino-Kenudson M: Update on large cell neuroendocrine carcinoma. *Transl Lung Cancer Res*. 2017;6:530–539.

26. Asamura H, Kameya T, Matsuno Y, et al. Neuroendocrine neoplasms of the lung: a prognostic spectrum. *J Clin Oncol*. 2006;24:70–76.

27. Marchevsky AM, Gal AA, Shah S, et al. Morphometry confirms the presence of considerable nuclear size overlap between “small cells” and “large cells” in high-grade pulmonary neuroendocrine neoplasms. *Am J Clin Pathol*. 2001;116:466–472.

28. Hiroshima K. Small cell carcinoma: distinction from large cell neuroendocrine carcinoma. In: Maldonado JG, Cervantes MK. editors. *Small Cell Carcinomas: Causes, Diagnosis and Treatment*. New York: Nova Science Publishers, 2009:101–121.

29. Kojima H, Watanabe R, Isaka M, et al. High-Grade Neuroendocrine Carcinoma with

Bronchial Intraepithelial Tumor Spread: Possibly a New Histologic Feature of Large-Cell Neuroendocrine Carcinoma. *J Thorac Oncol*. 2015;10:1337–1340.

30. Rosen Y. Pulmonary neuroendocrine carcinomas in situ: do they exist? *Histopathology*. 2022;80:627–634.

31. Minami K, Tanaka Y, Ogawa H, et al. Neuroendocrine marker staining pattern categorization of small-sized pulmonary large cell neuroendocrine carcinoma. *Thorac Cancer*. 2019;10:2152–2160.

32. Megyesfalvi Z, Barany N, Lantos A, et al, Expression patterns and prognostic relevance of subtype-specific transcription factors in surgically resected small-cell lung cancer: an international multicenter study. *J Pathol*. 2022;257:674–686.

33. Yamada Y, Belharazem-Vitacolonnna D, Bohnenberger H, et al. Pulmonary cancers across different histotypes share hybrid tuft cell/ionocyte-like molecular features and potentially druggable vulnerabilities. *Cell Death Dis*. 2022;13:979.

34. Goldfarbmuren KC, Jackson ND, Sajuthi SP, et al. Dissecting the cellular specificity of smoking effects and reconstructing lineages in the human airway epithelium. *Nat Commun*. 2020;11:2485.

35. Cheng H, Zhang Z, Rodriguez-Barrueco R, et al. Functional genomics screen identifies YAP1 as a key determinant to enhance treatment sensitivity in lung cancer cells. *Oncotarget*. 2016;7:28976–28988.

36. Wang Y, Dong Q, Zhang Q, et al. Overexpression of yes-associated protein contributes to progression and poor prognosis of non-small-cell lung cancer. *Cancer Sci*. 2010;101:1279–1285.

37. Horn, L, Mansfield AS, Szczesna A et al. First-Line Atezolizumab plus Chemotherapy in Extensive-Stage Small-Cell Lung Cancer. *N Engl J Med*. 2018;379:2220–2229.

38. Goldman JW, Dvorkin M, Chen Y, et al. Durvalumab, with or without tremelimumab, plus platinum-etoposide versus platinum-etoposide alone in first-line treatment of extensive-stage small-cell lung cancer (CASPIAN): updated results from a randomised, controlled, open-label, phase 3 trial. *Lancet Oncol*. 2021;22:51–65.

39. Owonnikoko TK, Niu H, Nackaerts K, et al. Randomized Phase II Study of Paclitaxel plus Alisertib versus Paclitaxel plus Placebo as Second-Line Therapy for SCLC: Primary and Correlative Biomarker Analyses. *J Thorac Oncol*. 2020;15:274–287.

40. Pietanza MC, Waqar SN, Krug LM, et al. Randomized, Double-Blind, Phase II Study of Temozolomide in Combination With Either Veliparib or Placebo in Patients With

Relapsed-Sensitive or Refractory Small-Cell Lung Cancer. *J Clin Oncol*. 2018;36:2386–2394.

Figure legends

1. Prognosis

(a,b) Comparing the four groups (SCLC- P, SCLC-non-P, LCNEC-P, and LCNEC-non-P), there was a significant difference in recurrence-free survival (RFS) (p=0.046), but no significant difference in overall survival (OS) (p=0.224). There were no significant differences in RFS and OS between SCLC-P vs. SCLC-non-P and LCNEC-P vs. LCNEC-non-P (c,d) Comparing NEC-P and NEC-non-P, there was a significant difference in recurrence-free survival (RFS) (p=0.026), but no significant difference in overall survival (OS) (p=0.172).

2. Graphic date of morphological features by seven types (refer to Table3 together)

(a) There are significant differences in cytomorphological score between SCLC-P vs. SCLC-non-P and LCNEC-P vs. LCNEC-non-P. Notably, the scatter dot plots showed an overlap between SCLC-P and LCNEC-P, and a larger difference between SCLC-non-P and LCNEC-non-P. (b-d) SCLC-P also exhibited features significantly more prominent in LCNEC, such as abundant stroma, nest formation, and comedo necrosis, suggesting difficulties separating SCLC and LCNEC. (e) Bronchial intraepithelial involvement was more frequently seen in SCLC-P than SCLC-non-P and LCNEC-P than LCNEC-non-P. (f) Background lung fibrosis was less in SCLC-P than SCLC-non-P. The red underbars in (a-c) indicated median values.

3. Representative pathological features

Typical SCLC-P, LCNEC-P, and LCNEC-A formed relatively round nests with comedo necrosis and a wider stroma with prominent inflammation, while typical SCLC-A showed a diffuse growth pattern with extensive coagulation necrosis.

Typical SCLC-A showed small cell cytology, and typical LCNEC-A showed non-small cell cytology. Typical SCLC-P and LCNEC-P exhibited intermediate cytomorphological features between SCLC and LCNEC. Most SCLC-A and LCNEC-A were negative for YAP1, while most SCLC-P and LCNEC-P were partially positive for YAP1.

4. Bronchial intraepithelial involvement in NEC-P

(a,b) Half of NEC-P showed bronchial intraepithelial involvement of tumor cells under the non-neoplastic ciliated epithelium. (c) One case of SCLC-P with intraalveolar involvement in one to several layers of tumor cells in non-neoplastic pneumocytes. (d) Double staining indicated that POU2F3-positive tumor cells (red) were present in the TTF-1-positive alveolar epithelium (blue).

5. Heatmap of IHC results (see Supplemental Digital Content 3 for details)

The heatmap of IHC clearly showed that SCLC-P and LCNEC-P shared a specific protein expression pattern (TTF-1^{low}, NE markers ^{low}, CEA ^{low}, YAP1 ^{high}, bcl-2 ^{high}, c-Myc ^{high}, and c-kit ^{high}). Conversely, there was a significantly different expression pattern between SCLC-

P vs. SCLC-non-P and LCNEC-P vs. LCNEC-non-P. For Rb1, 300 (yellow) indicated retain, and 0 (blue) indicated total loss. There was no significant difference in the frequency of Rb1 loss between SCLC-P and LCNEC-P; however, there was a significant difference between SCLC-non-P and LCNEC-non-P. For PD-L1, 300 (yellow) indicated positive (TPS >1%) , and 0 (blue) indicated negative.

6. Scatter plot of cytomorphological score and NE-score

Each case was plotted so that the cytomorphological score was on the horizontal axis (0–12) and NE-score (0–300) was on the vertical axis. SCLC-P was red squares, LCNEC-P was blue squares, SCLC-non-P was black circles, and LCNEC-non-P was green circles, with the respective 95% confidence intervals indicated by each colored thick solid line. The 95% confidence intervals for SCLC-P and LCNEC-P overlapped, while the 95% confidence intervals for SCLC-P and LCNEC-P have little overlap. The thin black lines showed the 95% confidence intervals for SCLC-A, SCLC-N, and SCLC-TN, and the thin green lines showed the 95% confidence intervals for LCNEC-A and LCNEC-TN. The distribution of SCLC-N is similar to that of SCLC-A, and the distribution of LCNEC-TN overlaps with that of LCNEC-P.

List of Supplemental Digital Content

1. Morphology review
2. Immunohistochemical protocol
3. Immunohistochemical results
4. Correlation coefficient (ρ) between novel transcriptional marker and each antibody

1.

Fig 1

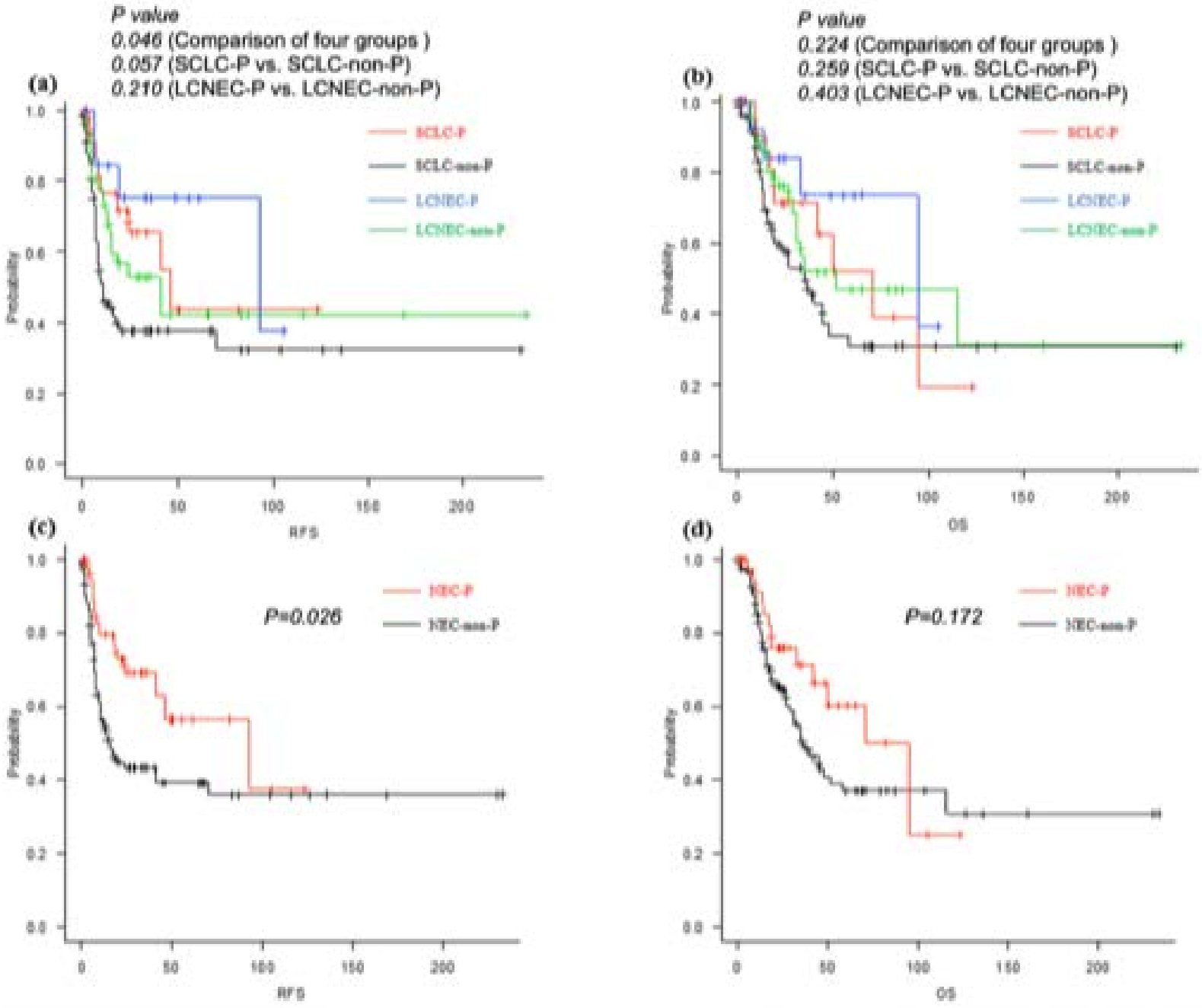
P value
0.046 (Comparison of four groups)
0.057 (SCLC-P vs. SCLC-non-P)
0.210 (LCNEC-P vs. LCNEC-non-P)
(a)
SCLC-P
SCLC-non-P
LCNEC-P
LCNEC-non-P
Probability
RFS
P value
0.224 (Comparison of four groups)
0.259 (SCLC-P vs. SCLC-non-P)
0.403 (LCNEC-P vs. LCNEC-non-P)
(b)
OS
(c)
P=0.026
(d)
P=0.172

Fig 2

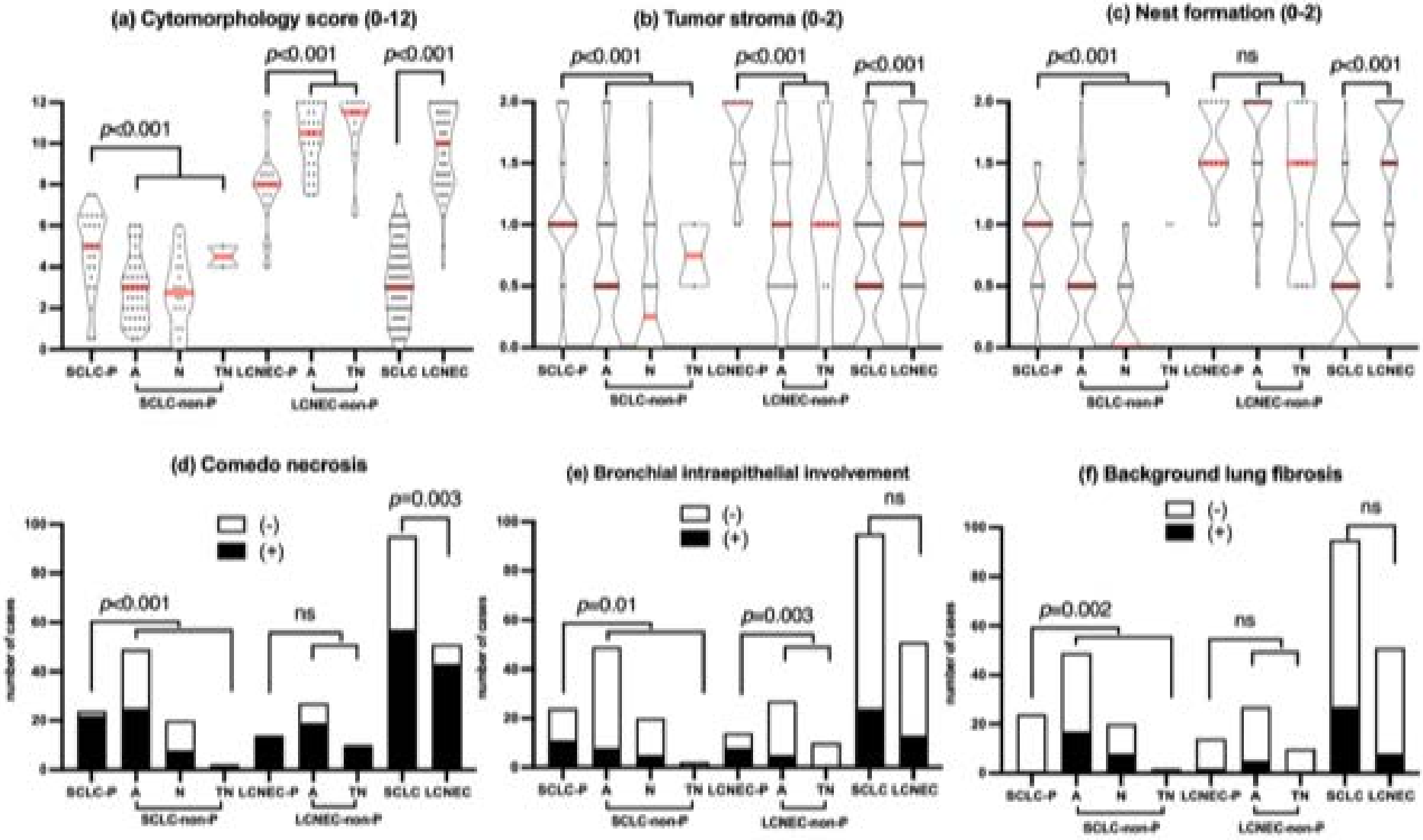
(a) Cytomorphology score (0-12)
p<0.001
p<0.001
p<0.001
SCLC-P
A
N
TN
LCNEC-P
A
TN
SCLC
LCNEC
SCLC-non-P
LCNEC-non-P
(b) Tumor stroma (0-2)
p<0.001
p<0.001
p<0.001
(c) Nest formation (0-2)
p<0.001
ns
p<0.001
(d) Comedo necrosis
(-)
(+)
p<0.001
ns
p=0.003
number of cases
(e) Bronchial intraepithelial involvement
p=0.01
p=0.003
ns
(f) Background lung fibrosis
p=0.002
ns
ns

Fig 3

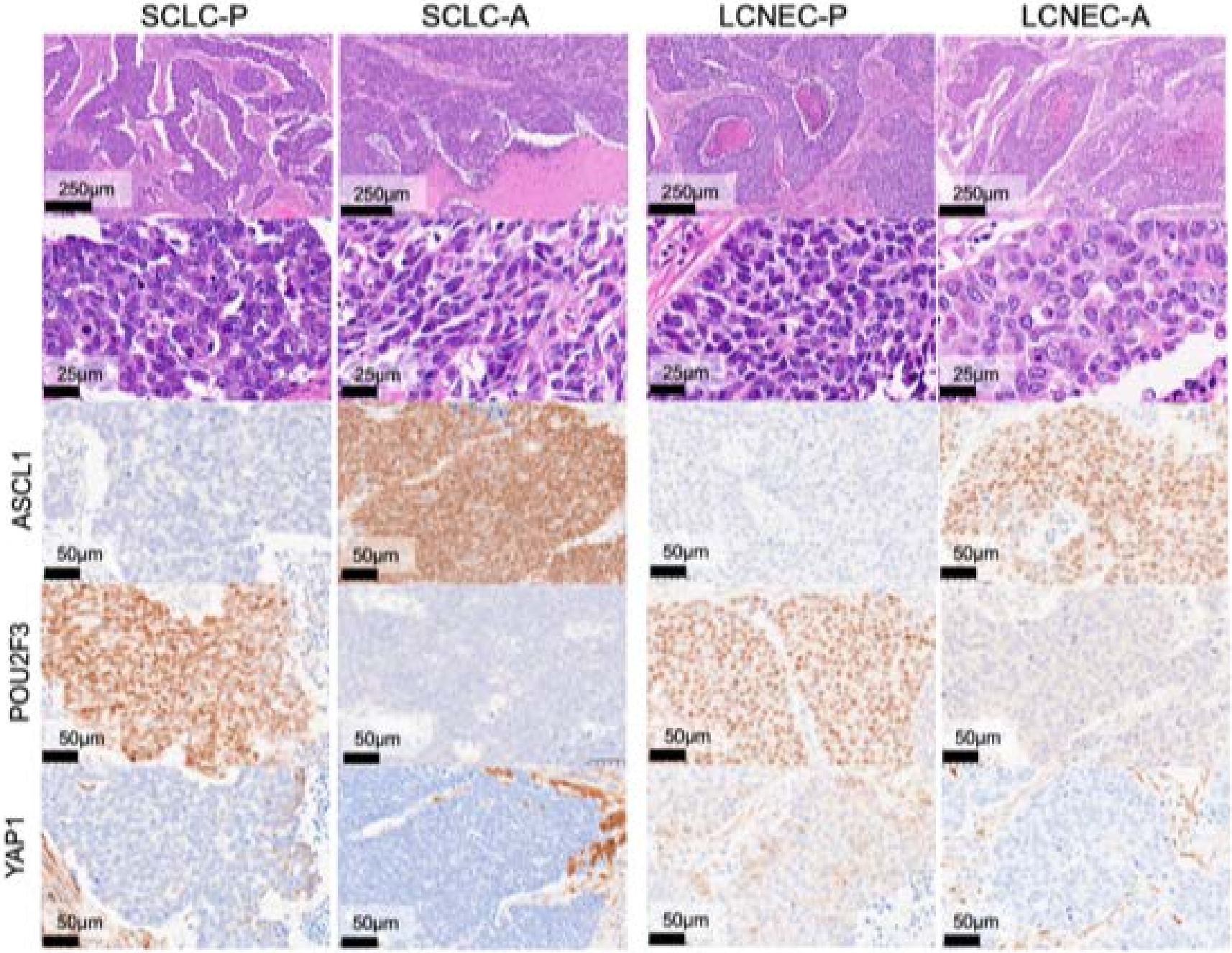
SCLC-P
SCLC-A
LCNEC-P
LCNEC-A
250μm
25μm
ASCL1
POU2F3
YAP1
50μm

Fig 4

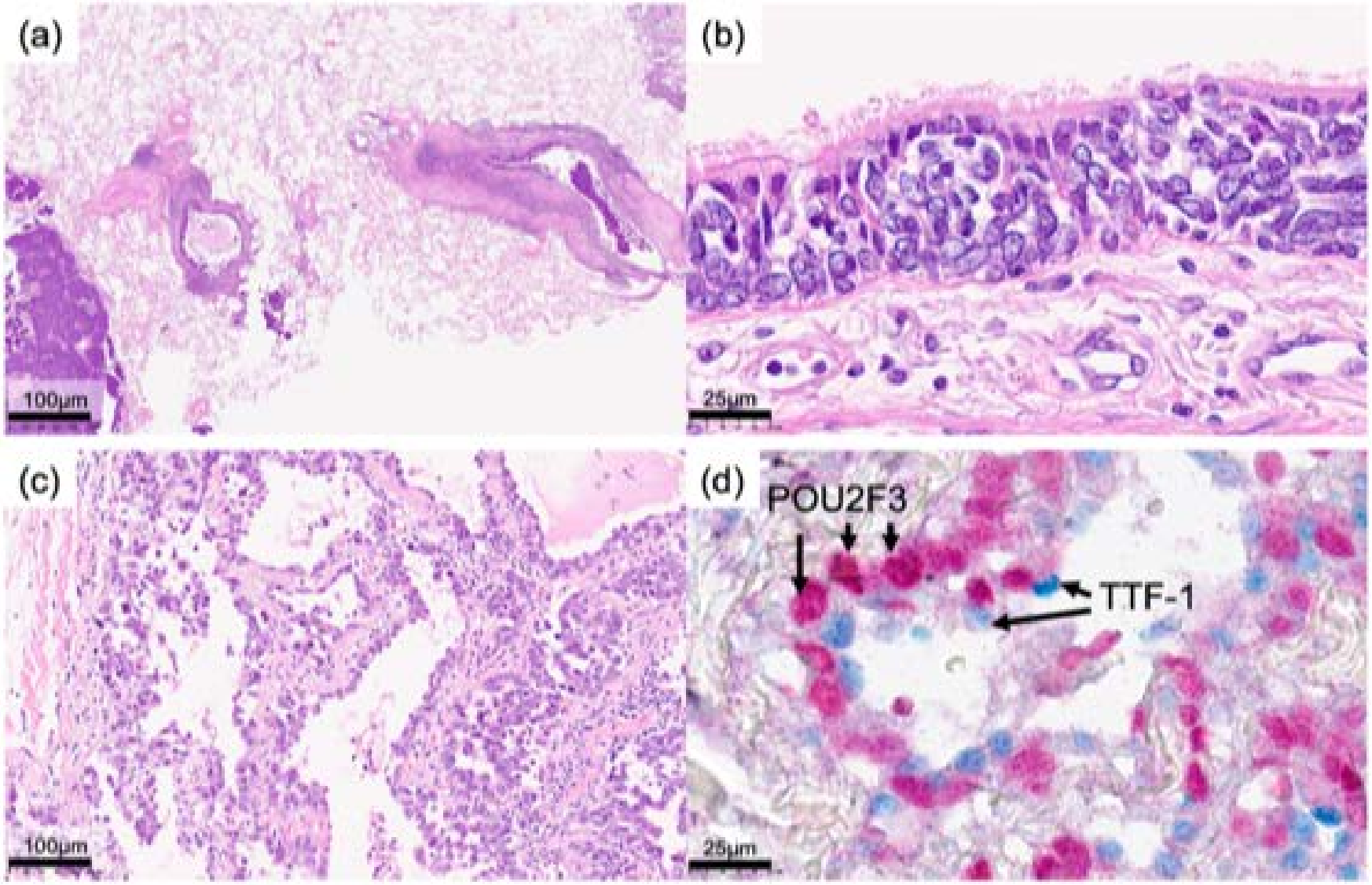

Fig 5

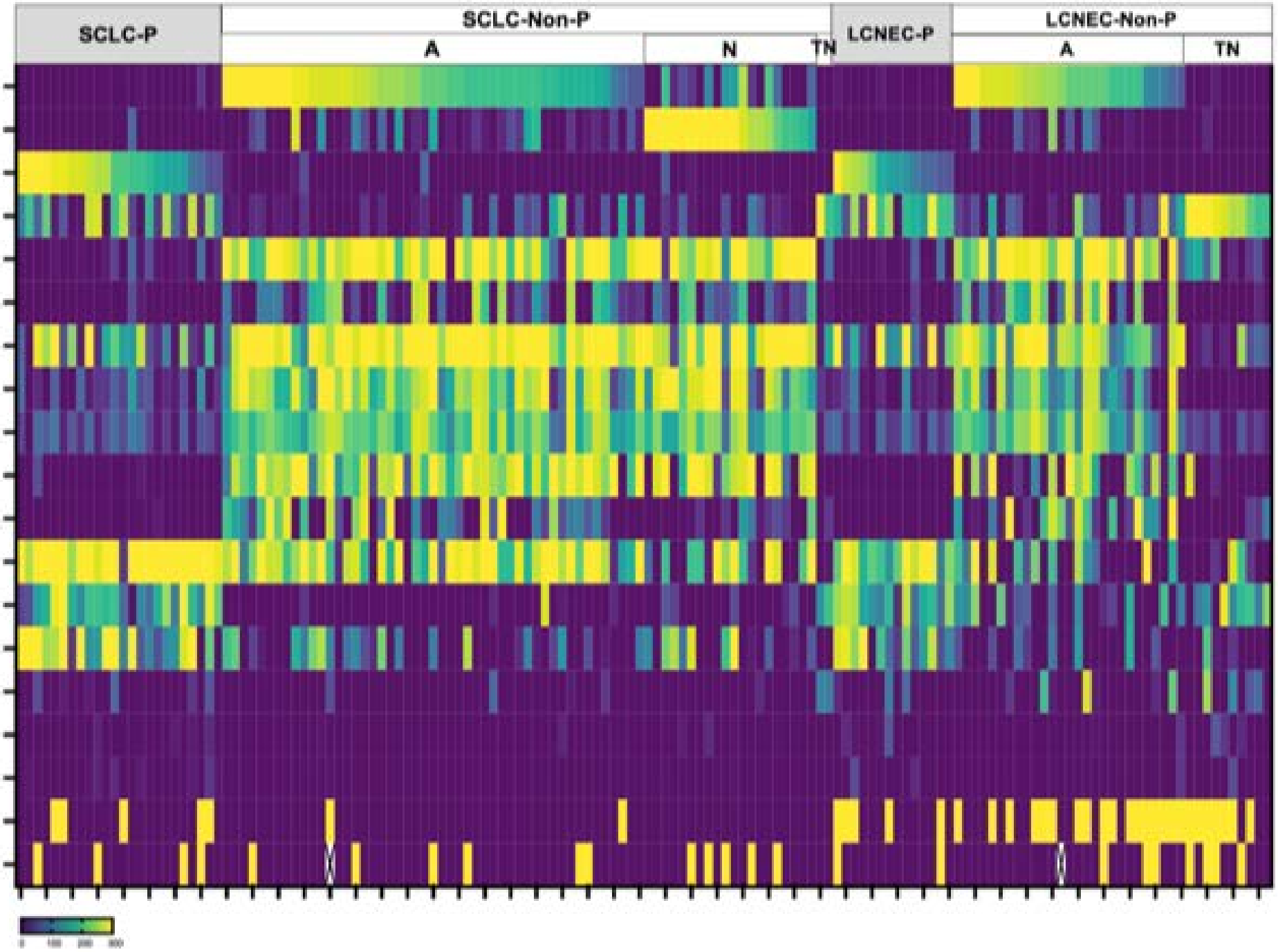
SCLC-P
SCLC-Non-P
A
N
TN
LCNEC-P
LCNEC-Non-P
A
TN
ASCL1
NEUROD1
POU2F3
YAP1
SYN
CGA
CD56
INSM
NE-score
TTF-1
CEA
bcl2
c-myc
c-kit
CD5
p40
CK5/6
Rb1
PD-L1

Fig 6

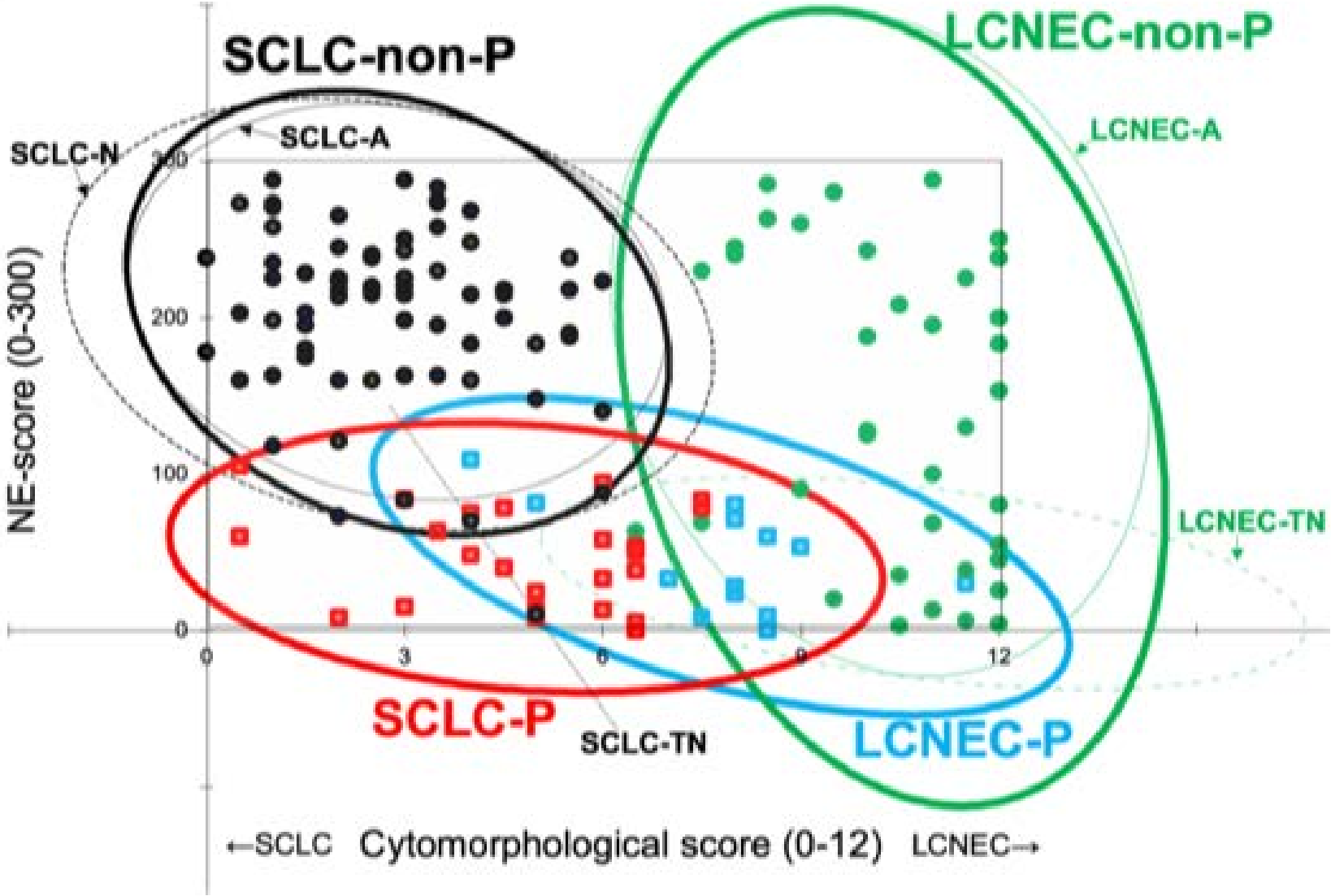
SCLC-non-P
LCNEC-non-P
SCLC-N
SCLC-A
LCNEC-A
NE-score (0-300)
200
100
0
LCNEC-TN
0
3
6
9
12
SCLC-P
SCLC-TN
LCNEC-P
←SCLC Cytomorphological score (0-12) LCNEC→

Table1: Group configuration and the number of cases in each group

SCLC (95)				LCNEC (51)			NEC (146)			
SCLC-P (24)	SCLC-non-P (71)			LCNEC-P (14)	LCNEC-non-P (37)		NEC-P (38)	NEC-non-P (108)		
	SCLC-A (49)	SCLC-N (20)	SCLC-TN (2)		LCNEC-A (27)	LCNEC-TN (10)		NEC-A (76)	NEC-N (20)	NEC-TN (12)

SCLC indicates small cell lung carcinoma; LCNEC, large cell neuroendocrine carcinoma; NEC, neuroendocrine carcinoma;
SCLC-P, SCLC dominantly expressing POU2F3; SCLC-non-P, SCLC other than SCLC-P; SCLC-A, SCLC dominantly expressing ASCL1;
SCLC-N, SCLC dominantly expressing NEUROD1; SCLC-TN, Triple-negative SCLC; LCNEC-P, LCNEC dominantly expressing POU2F3;
LCNEC-non-P, LCNEC other than LCNEC-P; LCNEC-A, LCNEC dominantly expressing ASCL1, LCNEC-TN, Triple-negative LCNEC;
NEC-P, NEC dominantly expressing POU2F3, NEC-non-P, NEC other than NEC-P; NEC-A, NEC dominantly expressing ASCL1;
NEC-N, NEC dominantly expressing NEUROD1; NEC-TN, Triple-negative NEC.

Table2: Patient characteristics

Features	SCLC (95)			LCNEC (51)			NEC (146)			SCLC (95)	LCNEC (51)	*P* value SCLC vs. LCNEC	Total (146)	*P* value SCLC-P vs. LCNEC-P	*P* value SCLC-non-P vs. LCNEC-non-P
	P (24)	non-P (71)	*P* value P vs. non-P	P (14)	non-P (37)	*P* value P vs. non-P	P (38)	non-P (108)	*P* value P vs. non-P						
Female, N (%)	2 (8%)	11 (15%)	ns	1 (7%)	6 (16%)	ns	3 (8%)	17 (16%)	ns	13 (14%)	7 (14%)	ns	20 (14%)	ns	ns
Age, median (range)	74 (61-88)	72 (40-89)	ns	75 (62-81)	70 (45-85)	ns	74 (61-88)	72 (40-89)	ns	73 (40-89)	72 (45-85)	ns	73 (40-89)	ns	ns
Smoking, median of pack-years (range)	54 (14-175)	50 (0-188)	ns	72 (20-300)	48 (0-200)	0.009	60 (14-300)	50 (0-200)	0.02	52 (0-300)	50 (0-188)	ns	51 (0-300)	ns	ns
Location, N (%)															
Peripheral	18 (75%)	54 (76%)	ns	9 (64%)	23 (62%)	ns	27 (71%)	77 (71%)	ns	72 (76%)	32 (63%)	ns	104 (71%)	ns	ns
Intermediate/Central	6 (25%)	17 (24%)		5 (36%)	14 (38%)		11 (29%)	31 (29%)		23 (24%)	19 (37%)		42 (29%)		
Pathological Stage, N (%)															
I	17 (71%)	30 (42%)	0.02	7 (50%)	18 (49%)	ns	24 (63%)	48 (44%)	ns	47 (49%)	25 (49%)	ns	72 (49%)	ns	ns
II-IV	7 (29%)	41 (58%)		7 (50%)	19 (51%)		14 (37%)	60 (56%)		48 (51%)	26 (51%)		74 (51%)		
Postpostoperative chemotherapy (+), N (%)	11 (46%)	41 (58%)	ns	4 (29%)	14 (38%)	ns	15 (39%)	55 (51%)	ns	52 (55%)	18 (35%)	0.04	70 (48%)	ns	ns
Combined histology with NSCLC (+), N (%)	5 (21%)	27 (38%)	ns	3 (21%)	13 (35%)	ns	8 (21%)	40 (37%)	ns	32 (34%)	16 (31%)	ns	48 (33%)	ns	ns
Combined histology with SQCC (+), N (%)	5 (21%)	14 (20%)	ns	3 (21%)	6 (16%)	ns	8 (21%)	20 (19%)	ns	19 (20%)	9 (18%)	ns	28 (19%)	ns	ns

N indicates number; NSCLC, non-small cell lung carcinoma; SQCC, squamous cell carcinoma; ns, not significant or $p > 0.05$, SCLC, small cell lung carcinoma; LCNEC, large cell neuroendocrine carcinoma; NEC, neuroendocrine carcinoma; SCLC-P, SCLC dominantly expressing POU2F3; SCLC-non-P, SCLC other than SCLC-P; LCNEC-P, LCNEC dominantly expressing POU2F3; LCNEC-non-P, LCNEC other than LCNEC-P, NEC-P; NEC dominantly expressing POU2F3; NEC-non-P; NEC other than NEC-P.

Table3: Morphological features

Features	SCLC (95)			LCNEC (51)			NEC (146)			SCLC (95)	LCNEC (51)	*P* value SCLC vs. LCNEC	Total (146)	*P* value SCLC-P vs. LCNEC-P	*P* value SCLC-non-P vs. LCNEC-non-P
	P (24)	non-P (71)	*P* value P vs. non-P	P (14)	non-P (37)	*P* value P vs. non-P	P (38)	non-P (108)	*P* value P vs. non-P						
Cytomorphological score, median score (range) (0-12)	5 (0.5-7.5)	3 (0-6)	<0.001	8 (4-11.5)	11 (6.5-12)	<0.001	6.3 (0.5-11.5)	4 (0-12)	ns	3 (0-7.5)	10 (4-12)	<0.001	5 (0-12)	<0.001	<0.001
Tumor stroma, median score (0-2)	1	0.5	<0.001	2	1	<0.001	1	0	<0.001	0.5	1	<0.001	1	0.0012	0.0019
Nest formation, median score (0-2)	1	0.5	<0.001	1.5	2	ns	1	0.5	0.012	0.5	1.5	<0.001	1	<0.001	<0.001
Comedo necrosis (+), N (%)	22 (92%)	35 (49%)	<0.001	14 (100%)	29 (78%)	ns	36 (95%)	64 (59%)	ns	57 (60%)	43 (84%)	0.003	100 (68%)	ns	0.004
Bronchial intraepithelial involvement (+), N (%)	11 (46%)	13 (18%)	0.01	8 (57%)	5 (14%)	0.003	19 (50%)	18 (17%)	<0.001	24 (25%)	13 (25%)	ns	37 (25%)	ns	ns
Background lung fibrosis (+), N (%)	1 (4%)	26 (37%)	0.002	2 (14%)	6 (16%)	ns	3 (8%)	32 (30%)	0.007	27 (28%)	8 (16%)	ns	35 (24%)	ns	0.029
Discussion for SCLC vs. LCNEC (+), N (%)	6 (25%)	3 (4%)	0.007	4 (29%)	3 (8%)	ns	10 (26%)	6 (6%)	0.002	9 (9%)	7 (14%)	ns	16 (11 %)	ns	ns

N indicates number; ns, not significant or $p > 0.05$; SCLC indicates small cell lung carcinoma; LCNEC, large cell neuroendocrine carcinoma; NEC, neuroendocrine carcinoma; SCLC-P, SCLC dominantly expressing POU2F3; SCLC-non-P, SCLC other than SCLC-P; LCNEC-P, LCNEC dominantly expressing POU2F3; LCNEC-non-P, LCNEC other than LCNEC-P, NEC-P; NEC dominantly expressing POU2F3; NEC-non-P; NEC other than NEC-P.